Topographic Effects on the Mean Tropospheric Flow Patterns around Antarctica

PETER G. BAINES

CSIRO Division of Atmospheric Research, Aspendale, Australia

KLAUS FRAEDRICH

Institut für Meteorologie, Freie Universitat Berlin, Berlin, West Germany

(Manuscript received 30 September 1988, in final form 3 March 1989)

ABSTRACT

Topographically induced flows around Antarctica in a rotating tank experiment with both homogeneous and stratified fluid are analyzed and compared with the mean tropospheric circulation. A circular tank of fluid was brought to a state of near-rigid clockwise rotation, and a topographic model of the Antarctic continent was then rotated counterclockwise to simulate a mean westerly zonal wind. Stratification was chosen to give the same ratios of topographic and dynamical length scales as in the atmosphere, as was the Rossby number based on the ratio of rotation rates. After the onset of the relative rotation of the Antarctic model, cyclonic eddies evolved in the coastal areas with, in the homogeneous case, anticyclonic eddies over the Antarctic dome. After about ten tank rotation periods, a dominant wavenumber 3 structure with cyclonic eddies in the Ross and Weddell seas and Prydz Bay is observed as an approximately steady state. Flow over the topography is relatively stagnant, with weak anticyclonic circulation. Variation of the Rossby number by a factor of 4 about the mean atmospheric value showed that the same general behavior was obtained, although there were differences in detail.

These flows show remarkable similarity to the observed mean 700 mb height and 850 mb wind fields around Antarctica. This strongly suggests that the same dynamical factors are operating, namely conservation of potential vorticity and strong coupling in the vertical, so that these motions are virtually barotropic. The large cyclonic eddies are then forced by flow separation around prominent coastal irregularities such as the Antarctic Peninsula.

1. Introduction

Studies of the mechanisms affecting Southern Hemisphere atmospheric flows have tended to emphasize the effects of the three mid-latitude continents (Africa, Australia and South America) while overlooking, perhaps, the effects of the fourth—Antarctica. Apart from the radiative and thermal effects of the ice and snow cover, Antarctica provides a massive asymmetrical barrier to this flow, rising steeply to heights greater than 3.5 km over much of its area (e.g., see the model in Fig. 1). Linear perturbation theory is not valid for atmospheric flow around topography of this magnitude under normal conditions (e.g., Baines 1987). In this paper we investigate the effects of this topography in a laboratory experiment. We first discuss the observed mean flow patterns in the atmosphere around Antarctica. We then describe some results of experiments for a range of conditions, some of which are dynamically very similar to those of the atmosphere. The correspondence between the two sets of flow patterns is remarkable, and leads to the inference that the structure seen in the atmosphere is principally forced by the effect of the Antarctic topographic barrier on a mean zonal flow.

Recently, Boyer and Chen (1987) have made a detailed laboratory study of the effects of topography on the mean Northern Hemisphere circulation. The relevance of some aspects of this study to the atmosphere has been questioned by James (1988b) because of a lack of spherical geometry and baroclinic effects. We believe that these criticisms are not applicable to the present study because the effects modeled are mostly at high latitudes, and the important effects described are largely barotropic.

2. Atmospheric flow patterns

The weather of the Antarctic is notoriously variable, and may change dramatically in a very short time (Schwerdtfeger 1984). However, some of its important features are persistent and fairly steady. One such example is the shallow katabatic winds that drain off the continent for much of the year. Another is the averaged tropospheric pressure patterns, which show a pronounced structure of three offshore lows, with a high centered over the eastern hemisphere of the continent. Figures 2a and 2b show the heights of the 700 mb pres-

Corresponding author address: Dr. Peter G. Baines, CSIRO Division of Atmospheric Research, Private Bag No. 1, Mordealloc, Vic. 3195, Australia.

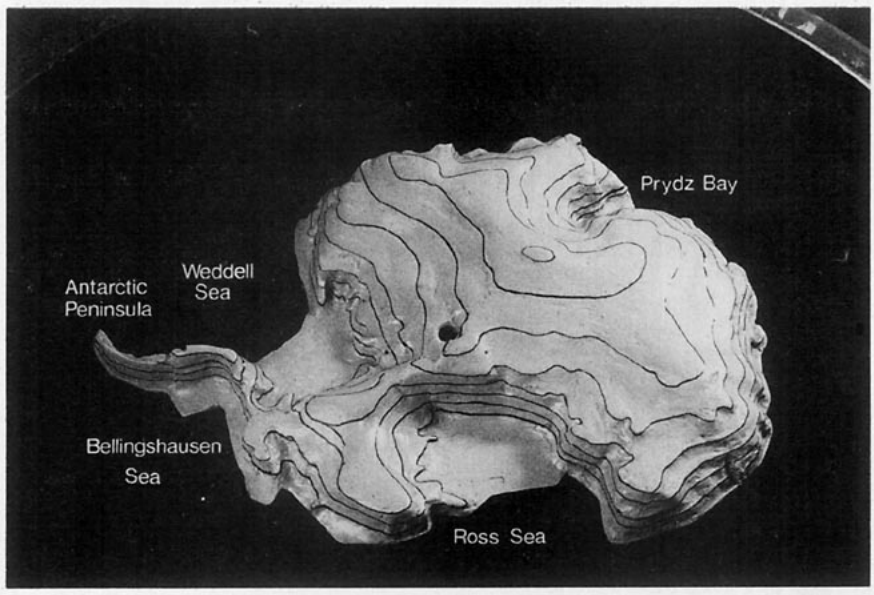

FIG. 1. A model of Antarctica used in the laboratory experiments. Height contours are shown in black, at intervals of 1 cm (≈500 m in the atmosphere). The diameter of the model is approximately 60 cm, and the dark hole denotes the South Pole.

sure surface for 10-year means for summer (December, January, and February) and winter (June, July, and August) respectively, taken from the "atlas" compiled by Le Marshall et al. (1985). Figure 3 shows the height of the 700 mb pressure surface for January taken from Hofmeyr (1957). In spite of the different periods and the relatively smaller quantity of data, Fig. 3 is very similar to Fig. 2a. As height increases, these pressure patterns become weaker and less distinct, with very little change in phase (Le Marshall et al. 1985). The pattern therefore extends through most of the troposphere, and is substantially barotropic.

Figure 4 shows the mean wind fields for winter for the 10-year period at 850 mb (the corresponding diagram for summer is very similar). Note that the winds are weak in the low-pressure regions shown in Figs. 2 and 3, poleward of the northernmost extent of the Antarctic topography, and are significantly larger at latitudes 60°S and less. Also, there are almost no changes in the mean flow pattern between the extreme seasons except for the rise and fall of the overall magnitude in geopotential height. Monthly mean flows have also been described by Jenne et al. (1974) using different data. Their results are similar to those shown here, although the circulation in the Weddell Sea is more pronounced, as in Fig. 3.

How representative are these means of the real flow field? An examination of the standard deviations of daily values of the height field for 700 mb and zonal wind components for 850 mb for both summer and winter (Fig. 5) shows that the contours of constant variance are much more zonal than the mean fields in each case. Hence, although the standard deviation of the zonal wind is generally comparable with the spatial variations in the mean, they will not affect the pattern shown by the mean values (Figs. 2 to 4) which is therefore highly significant.

To our knowledge, no clear explanation has yet been advanced for the occurrence of this persistent mean flow pattern. Schwerdtfeger (1984) displays mean-sea-level pressure patterns (his Figs. 4.1a and 4.1b) which show the same structure as Figs. 2 and 3 here, but he gives no explanation for these patterns and seems to imply that they are caused by migrating cyclones.

It seems likely that a dominant factor causing this mean circulation is the Antarctic topography; the three lows correspond well with the Weddell and Ross seas and Prydz Bay, and form a near-symmetric wavenumber 3 structure which will be discussed later. Apart from the cyclonic storms from lower latitudes, other local processes are not expected to generate strong large-scale synoptic systems: the near uniform and large albedo of the snow and ice-covered surfaces implies that thermal forcing of atmospheric circulation by surface fluxes is weak (except, possibly, at the edge of the pack ice), and the low moisture content of the air implies that latent heat processes are also small.

Studies of the zonally averaged properties of atmospheric winds show that small but persistent westerly zonal flow exists in southern polar regions. Figure 6, taken from Trenberth (1979), shows a mean westerly zonal wind of about 5 m s^{-1} at 70°S, decreasing polewards in a linear fashion with approximately uniform vorticity. Outside this region, monthly mean winds in

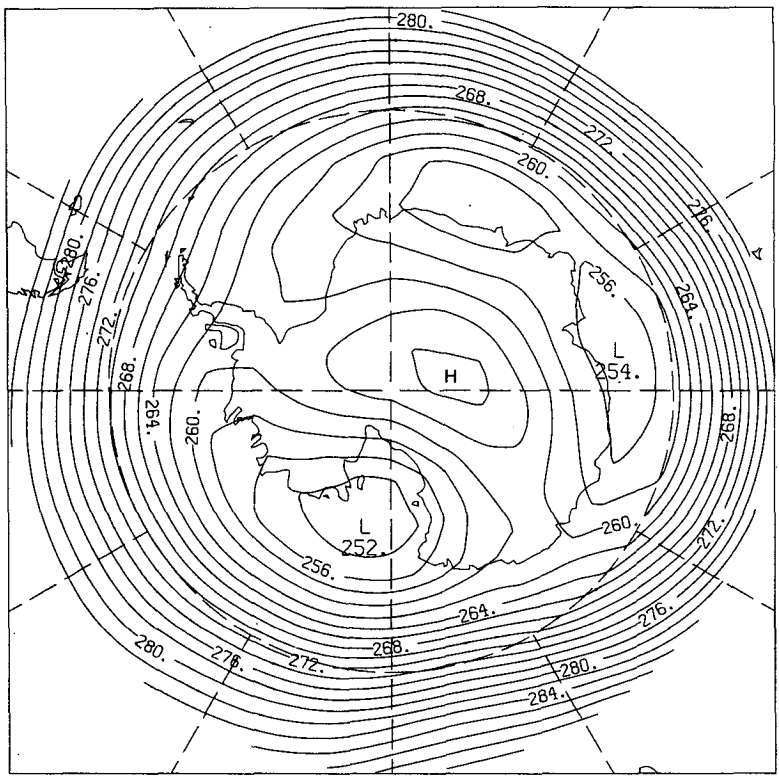

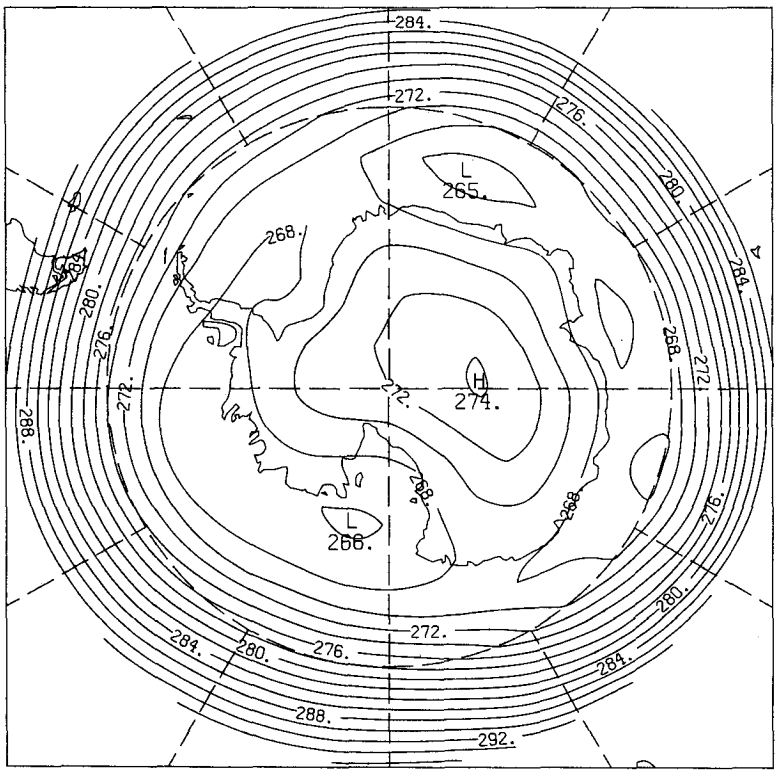

FIG. 2. Mean 700 mb geopotential height field over Antarctica in decameters in (a) winter (June–July–August, JJA) and (b) summer (December–January–February, DJF) from the dataset of Le Marshall et al. (1985). Contour intervals are 2 dam.

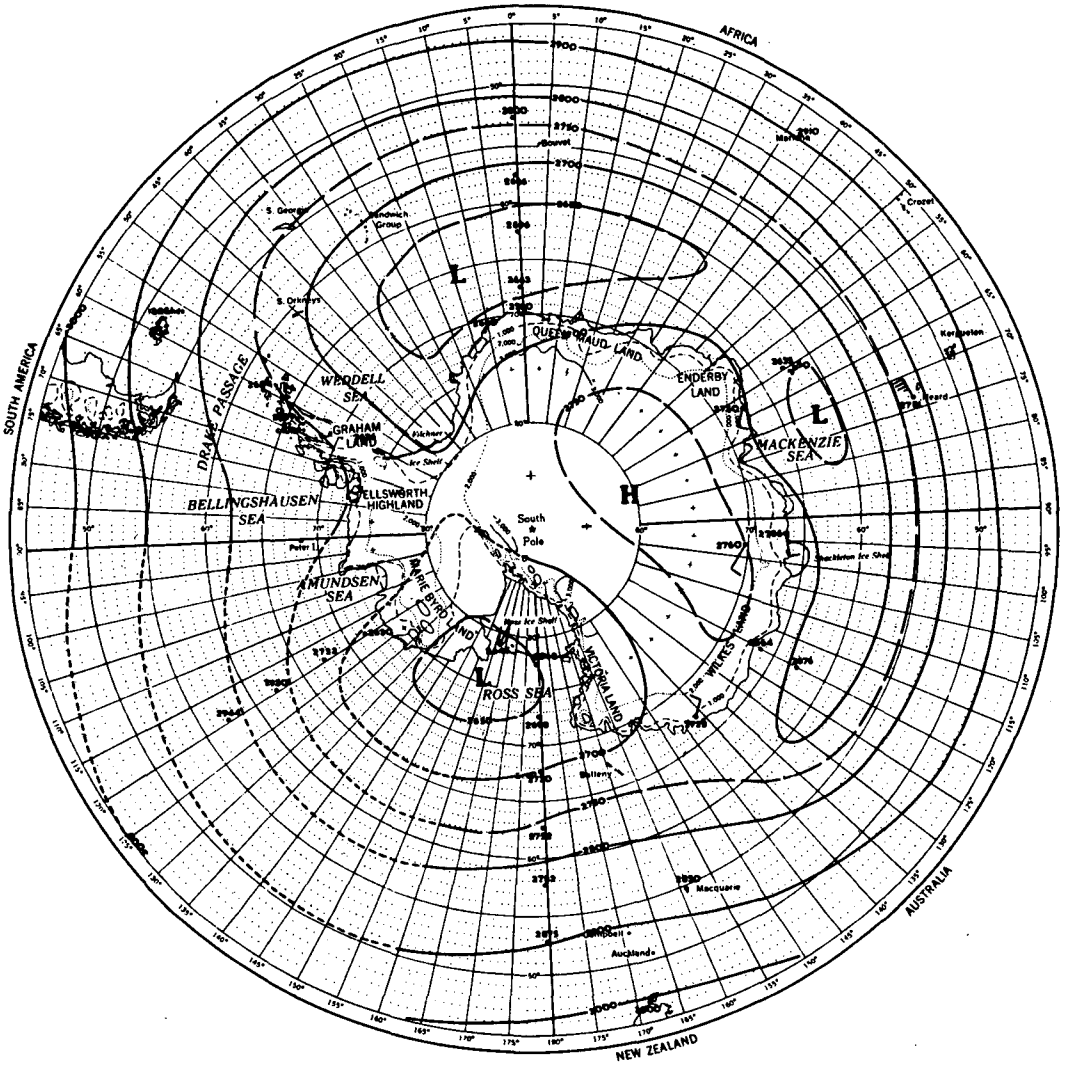

FIG. 3. Mean 700 mb geopotential height contours for January, from Hofmeyr (1957). Contour intervals are 50 m.

the latitude range 50°S to 65°S are predominantly zonal westerlies, and increase monotonically with height. The mean value U for the seasonal means generally satisfies

$$U = u(500 \text{ mb})$$

$$\approx \frac{1}{2}[u(1000 \text{ mb}) + u(300 \text{ mb})]. \quad (2.1)$$

We shall therefore consider a simple model consisting of a cyclonic polar-centered vortex interacting with the topography of Antarctica for our laboratory simulations.

3. A laboratory model

A laboratory model of Antarctica was constructed at Aspendale (by Mr. David Murray), with a height scale of 2 cm/1000 m, and a horizontal scale of 11.25 cm/1000 km, giving a maximum height $h(\max)$ of 8 cm and a maximum horizontal radius of 32.5 cm (Fig. 1). The tank was filled to a depth D of approximately 22 cm, so that the ratio $h(\max)/D$ was approximately equal to the atmospheric value if D corresponds to the depth of the troposphere. The model was placed centrally in a circular tank of diameter 110 cm, mounted on a rotating turntable. The turntable was rotated in a clockwise sense (Southern Hemisphere rotation), with typical rotation periods of about 4 seconds. The Antarctic model was mounted so that it could be rotated independently about the polar axis. In most experiments it was rotated in an anticlockwise sense relative to the tank, to simulate a mean westerly zonal wind field with uniform vorticity.

Experiments were done with two types of fluids: ho-

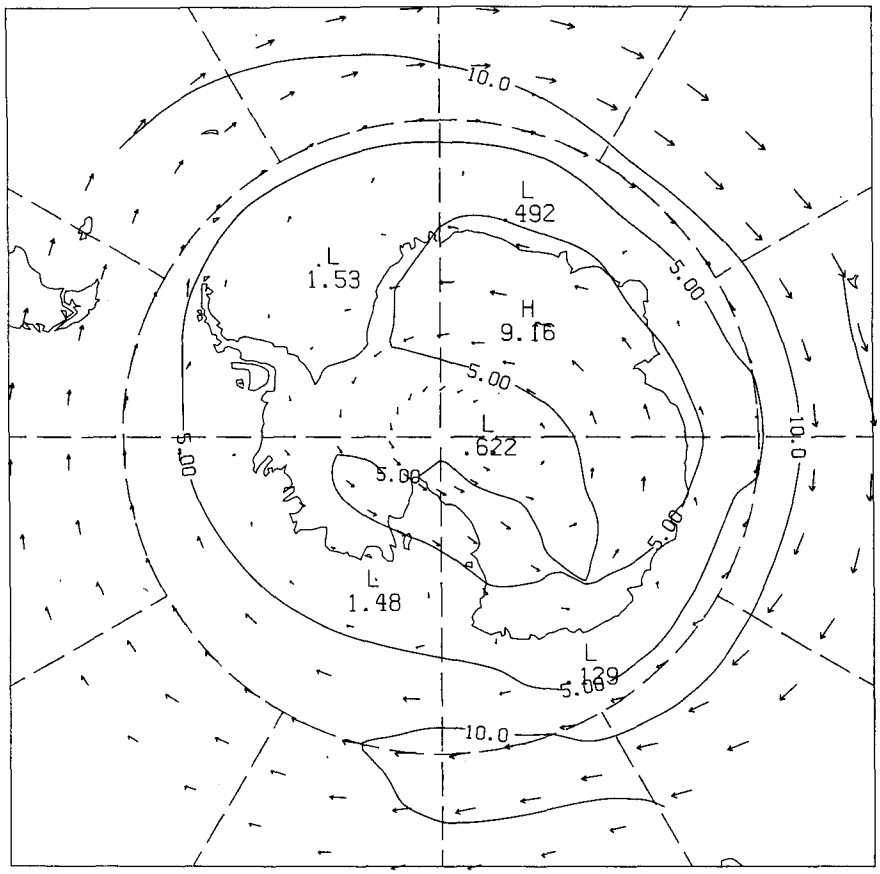

FIG. 4. Mean 850 mb wind field in m s^{-1} in winter (JJA) from the dataset of Le Marshall et al. (1985). Contour intervals are 5 m s^{-1}.

mogeneous fluid (fresh water), and a stably stratified fluid with constant buoyancy frequency N. Two techniques of flow visualization were used. In the first, used with homogeneous fluid, radially located rakes which released colored dye at various latitudes were inserted into the tank and attached to the framework that supported the obstacle, so that they rotated with it. This was eventually discarded in favor of the second technique which was used with both homogeneous and stratified fluids. It involved placing a large number of neutrally buoyant (or in the case of homogeneous fluids, nearly neutrally buoyant) beads in the fluid, and illuminating the tank with a thin horizontal beam of light produced by a laser, at some particular level. Data were recorded photographically by a camera that looked vertically downward from above the model and rotated with it. Fluid velocities could be determined by the measurement of lengths of streaks produced by the beads in the time-exposure photographs. The stratified case is more representative of the atmospheric situation, but the homogeneous fluid may be used as a model for the barotropic flow in the atmosphere, and the comparisons are interesting.

For the homogeneous fluids, for each run described here the tank was allowed to rotate for at least 1 hour to attain a state of rigid rotation before the relative motion of the topography was commenced. For the stratified runs, the tank was filled while rotating via fluid slip rings using the customary two-tank technique. Once filled, it was left for a period of 1 hour or more to approach steady state. Spinup of stratified fluids is a poorly explored topic, and steady state may not be attainable in many situations because of the Sweet–Eddington circulation (Griffiths and Linden 1985) and other poorly understood processes. The experience at Aspendale has been that weak residual motion persists even after many hours of steady conditions. The velocities are much smaller than those forced by the topography in the present experiments, and we must assume they are too weak to affect the results described here.

Two important dynamical parameters for these phenomena are the Ekman number E and the Rossby number Ro, defined respectively by

$$E = \nu/2\Omega a^2, \quad \mathrm{Ro} = U/2\Omega L, \qquad (3.1)$$

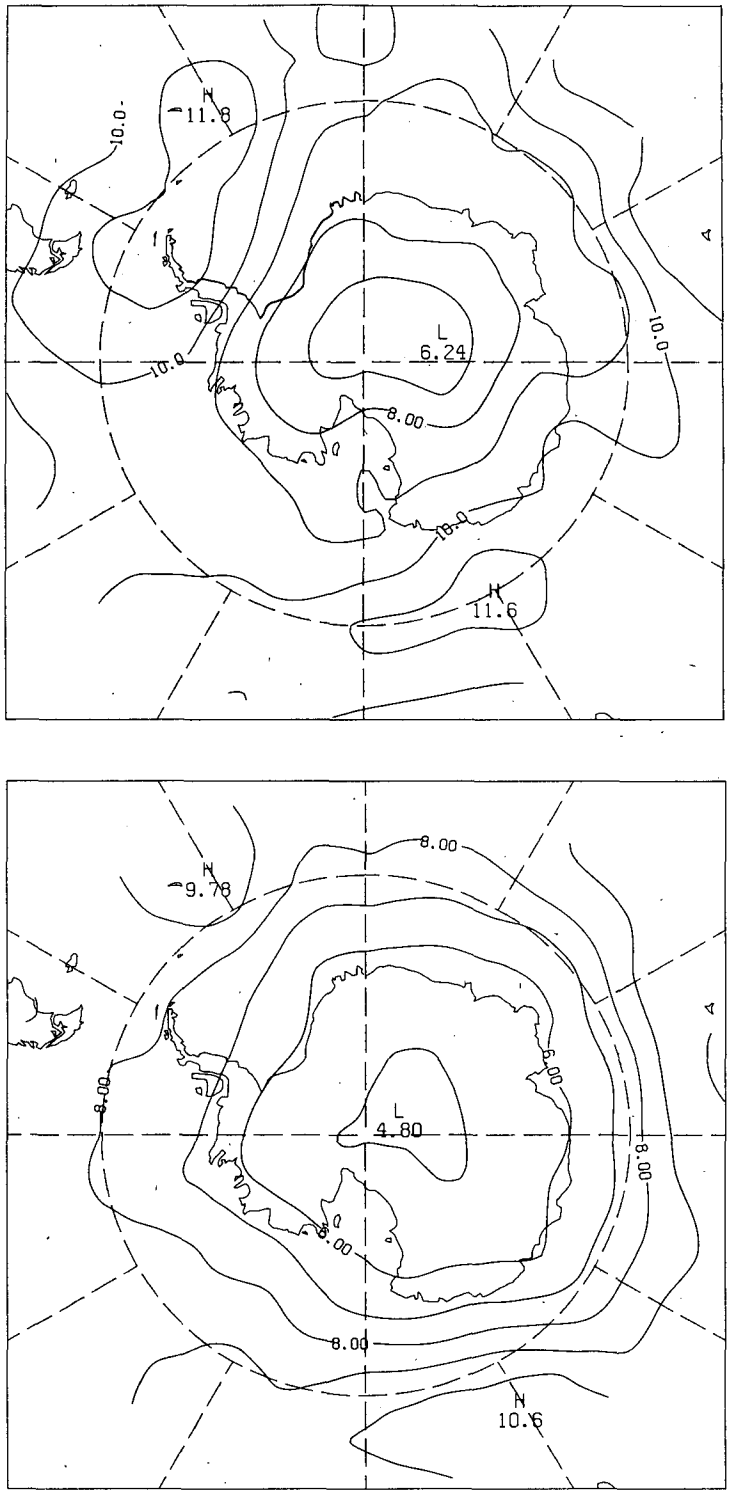

FIG. 5. Standard deviations of daily 700 mb geopotential heights in decameters for (a) winter (JJA) and (b) summer (DJF), and standard deviations of daily zonal wind components at 850 mb for (c) winter (JJA) and (d) summer (DJF), from the dataset of Le Marshall et al. (1985). Contour intervals are 1 dam and 1 m s^{-1}, respectively.

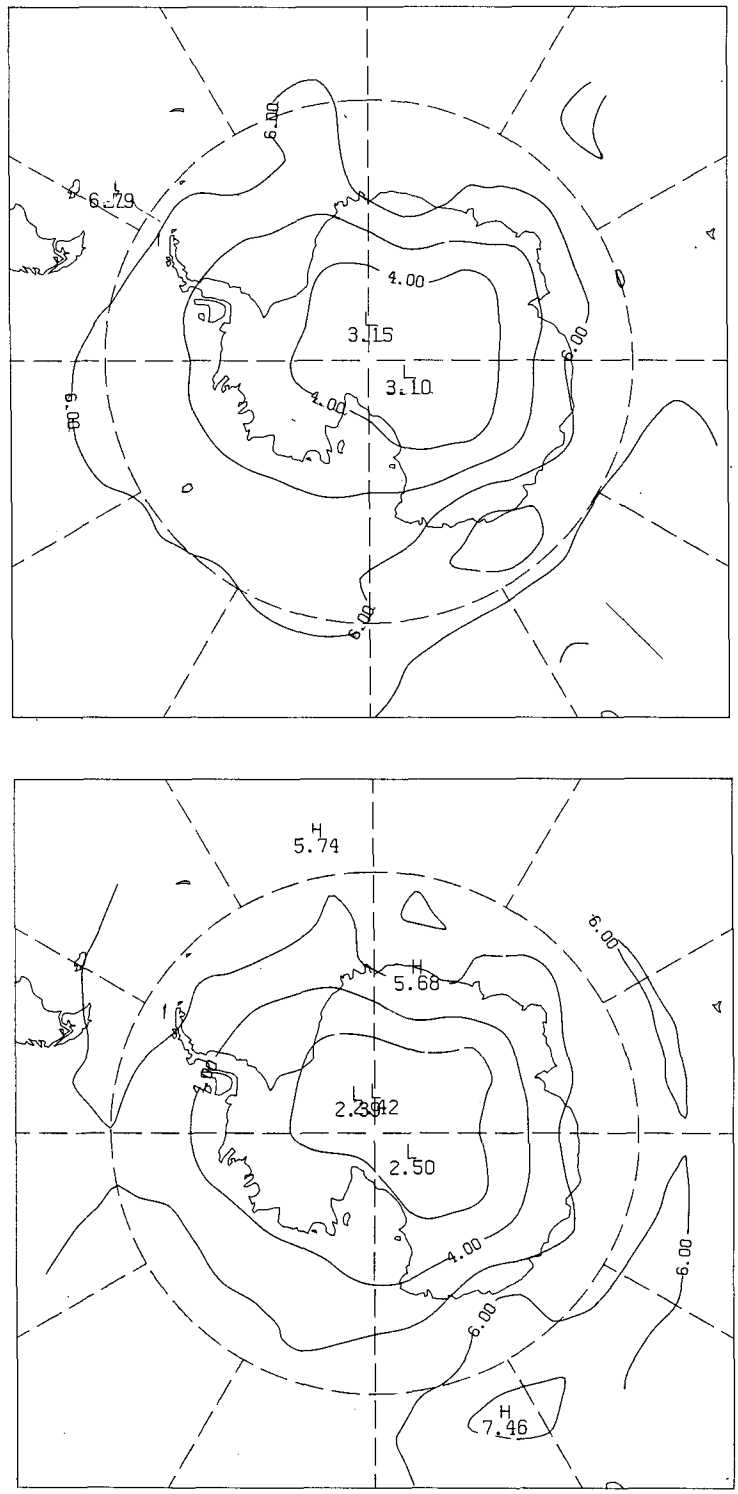

FIG. 5. (*Continued*)

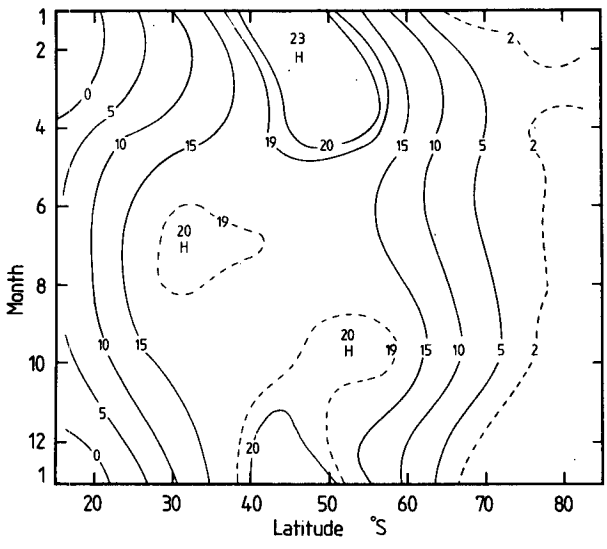

FIG. 6. The mean annual cycle of the zonally averaged westerly component of geostrophic wind at 500 mb in m s^{-1} as a function of latitude and month (from Trenberth 1979).

where a is a representative radius of Antarctica, Ω is the angular velocity of the earth, L denotes a length scale for the indentations of the Antarctic topography, ν is the kinematic viscosity, and U is a mean zonal speed. We therefore have $U = \omega a$, where ω is the angular velocity of the topographic model, and

$$\mathrm{Ro} = \left(\frac{a}{2L}\right)\left(\frac{\omega}{\Omega}\right). \tag{3.2}$$

With a rotation period of $2\pi/\Omega$ of 4 seconds, $a = 30$ cm, $a/L = 3$, and $\omega/\Omega = 0.03$ in the laboratory, we have

$$E = 4 \times 10^{-6}, \quad \mathrm{Ro} = 0.045, \tag{3.3}$$

so that both are small and $E^{1/2} \ll \mathrm{Ro}$. The latter condition implies that viscous effects are much smaller than inertial effects in these experiments (Baines and Davies 1980), as is required in order to model the atmosphere.

For homogeneous fluids, under the above conditions the fluid motion has very little horizontal shear, and potential vorticity is conserved even for topography with steepness of order unity. Hence the governing equation for the homogeneous experiments is

$$\frac{d}{dt}\left(\frac{\zeta + 2\Omega}{D - h}\right) = 0, \tag{3.4}$$

where ζ is the vorticity relative to axes rotating with the topography, and D is the fluid depth, given by

$$D = D(0) + \Omega^2 r^2/2g. \tag{3.5}$$

Here $h(r, \theta)$ is the topographic height, and r, θ are polar coordinates. This configuration simulates a polar beta plane for bartotropic motion but, as in the atmosphere, this beta effect is small in comparison with the corresponding effect of the Antarctic topography. With these conditions, the only externally controlled dimensionless variable in the experiments is the ratio ω/Ω, where Ω is the angular velocity of the Antarctic model. In the atmosphere $\omega/\Omega \sim 0.03$.

For this vorticity-based dynamics, the appropriate degree of vertical stretching of the topographic model may be estimated as follows. With x eastward and y northward Cartesian coordinates and u and v corresponding velocities, a streamfunction ψ may be defined by

$$(D - h)u = -\partial\psi/\partial y, \quad (D - h)v = \partial\psi/\partial x. \tag{3.6}$$

If h is assumed to be a function of y only, the linearized form of equation 3.4 is

$$\frac{\partial}{\partial t}\left[\nabla^2\psi + \left(\frac{\partial\psi}{\partial y}\frac{dh}{dy}\right)(D - h)^{-1}\right] + 2\Omega\left(\frac{\partial\psi}{\partial x}\frac{dh}{dy}\right)(D - h)^{-1} = 0. \tag{3.7}$$

For waves over the topographic escarpment we write $\psi \sim \exp i(kx + ly + \omega t)$, and with $k^2 \ll l^2$, $L_y/|dh/dy|/(D - h) < 1$, we obtain

$$\frac{\omega}{\Omega} \sim \frac{dh/dy}{\pi(D - h)}\frac{L_y^2}{L_x}, \tag{3.8}$$

where $k = 2\pi/L_x$, $l = 2\pi/L_y$. Taking L_y as the width of the sloping topography so that $dh/dy \sim \Delta h/L_y$ where Δh is the height of the top of the escarpment,

$$\frac{\omega}{\Omega} \sim \frac{1}{\pi}\frac{L_y}{L_x}\frac{\Delta h}{D}. \tag{3.9}$$

In the atmosphere we have $\Delta h/D \sim 3$ km/8 km, and in the laboratory $\Delta h/D \sim 6$ cm/20 cm. The similarity of these ratios guarantees that the vortex stretching effect and the Rossby wave frequencies scale appropriately.

The importance of the beta effect away from the topography may be estimated by comparing the vorticity gradient of the fluid with the planetary vorticity. For the atmosphere, at 70°S we have

$$\frac{\partial\zeta}{\partial r}\beta^{-1} \sim \frac{U}{La\beta} = \left(\frac{U}{2\Omega L}\right)\left(\frac{A}{a\sin 20°}\right) = \frac{\omega}{\Omega}\frac{A}{2L\sin 20°}, \tag{3.10}$$

where A is the Earth's radius, and for latitude 70°S we have $U = 5$ m s^{-1}, $a = 2200$ km, and $L = 700$ km, we obtain a value of 0.43. For the laboratory, with a homogeneous fluid with a sloping free surface, the term corresponding to β is $2\Omega^3 a/gD$, and at radius a we

have

$$\frac{\partial \zeta}{\partial r}\left(\frac{2\Omega^3 a}{gD}\right)^{-1} \sim \frac{U}{2L\Omega}\frac{gD}{\Omega^2 a^2} = \frac{\omega}{\Omega}\frac{gD}{\Omega^2 2La}, \quad (3.11)$$

and with $\omega/\Omega = 0.03$, $D = 24$ cm, $a = 30$ cm, and $L = 10$ cm, we obtain a value of 0.47. In both cases therefore the "beta effect" is significant, and has the same relative magnitude with these parameter values.

For fluids where the stratification is significant, it is customary to use the quasi-geostrophic equations to describe the dynamics, with the conservation of quasi-geostrophic potential vorticity (e.g., Gill 1982, p. 530). However, this is only applicable for linearized topography; for high or steep topography, other phenomena such as low-frequency Kelvin waves (which are only geostrophic in one direction) may occur. Theoretical models for these cases with realistic topography are cumbersome. The equation corresponding to Eq. 3.4 is the conservation of Ertel's potential vorticity

$$\frac{d}{dt}\left((\zeta + 2\Omega)\cdot\frac{\nabla\rho}{\rho}\right) = 0, \quad (3.12)$$

where ρ is the density field and ζ and Ω are vector quantities. This equation is exact for inviscid flow (Pedlosky 1979).

Stratification introduces the additional parameter N, the buoyancy frequency. For stratified flows in the atmosphere on short time scales where rotation is not important, fluid approaching a topographic barrier will be blocked upstream at low levels if (e.g., Baines 1987)

$$\frac{Nh_m}{U} > 2. \quad (3.13)$$

In the atmosphere, with $N = 10^{-2}$ s, $h_m = 3$ km, and $U = 5$ m s^{-1}, this criterion is easily satisfied for Antarctica. For motions on synoptic time scales the situation is different. Assuming that the total depth scale of the atmosphere or tank is not important, the significant dimensionless parameters may be written as Ro, a/L, and $Nh_m/2\Omega L$. This last quantity may be written

$$\frac{Nh_m}{2\Omega L} = \left(\frac{U}{2\Omega L}\right)\left(\frac{Nh_m}{U}\right), \quad (3.14)$$

and is the ratio of the topographic height to the height scale of motions with horizontal length L. In the atmosphere this has a value of about 0.2, so that disturbances with $L > 700$ km have a height scale greater than the depth of the troposphere. In the laboratory experiments we equate the values of these numbers with those of the atmosphere.

4. Experimental observations and results

Our end goal in this study is to provide a conceptual explanation for the mean flow patterns around Antarctica. We base this explanation on a visual comparison between the laboratory and atmospheric flow patterns. More quantitative comparisons are difficult at this stage, and visual inspection is often the best technique for recognizing meaningful structures and similarities.

a. Barotropic experiments

Experiments were conducted with homogeneous fluid for values of $\omega/\Omega = 0.015$, 0.03, and 0.06. The fluid was allowed to reach an approximate state of rigid rotation, and then the relative motion of Antarctica was commenced at time $t = 0$. Flow patterns at a level of 8 cm (approximately), just above the maximum topographic height are shown in Fig. 7 for the case $\omega/\Omega = 0.03$, which corresponds to the mean atmospheric zonal wind obtained from Fig. 6. Figures 7a to 7f show the development of the flow after the commencement of motion, from 3 days to a month. Large persistent eddies develop in three prominent locations (Weddell Sea, Ross Sea, and Prydz Bay), and a substantial number of rapidly varying small-scale cyclonic eddies may be seen. These are mostly close to the boundaries of the topography, or they tend to move towards it. Eddies formed in the coastal indentations tend to remain stationary. Over the eastern hemisphere of Antarctica, one or two anticyclonic eddies are observed. Note the pronounced effect of the Antarctic Peninsula in deflecting the flow.

As time progresses, the large eddies forming in the Weddell and Ross seas become the dominant features of the flow pattern; the smaller cyclonic eddies do not vanish, but the anticyclonic eddies over the continent become progressively weaker. Figure 7g represents an approximate steady state, which is approximately reached after $t = 60$ s. In this flow state, the fluid over the topography is relatively quiescent, as might be expected from conservation of potential vorticity: in the steady state the flow tends to follow the height contours. Note that the presence of the offshore eddies generally results in flow with an "easterly" component in the coastal regions at most longitudes. This implies a broad anticyclonic region over the topography.

Casual inspection of the flow properties at other heights indicated that the flow there was quite similar. This is partly visible in the photographs of Fig. 7. The sharply focused streaks denote the level of the laser beam; less well-defined, duller streaks denote beads on the upper free surface of the fluid. The latter show a very similar flow pattern to that at low levels; the eddies at the upper level appear to be slightly displaced from those at the lower levels, but this is probably largely due to parallax in many cases, as the eddies at the upper level are generally seen to be displaced radially outward relative to their counterparts at the lower level.

Similar behavior is observed for the other parameter

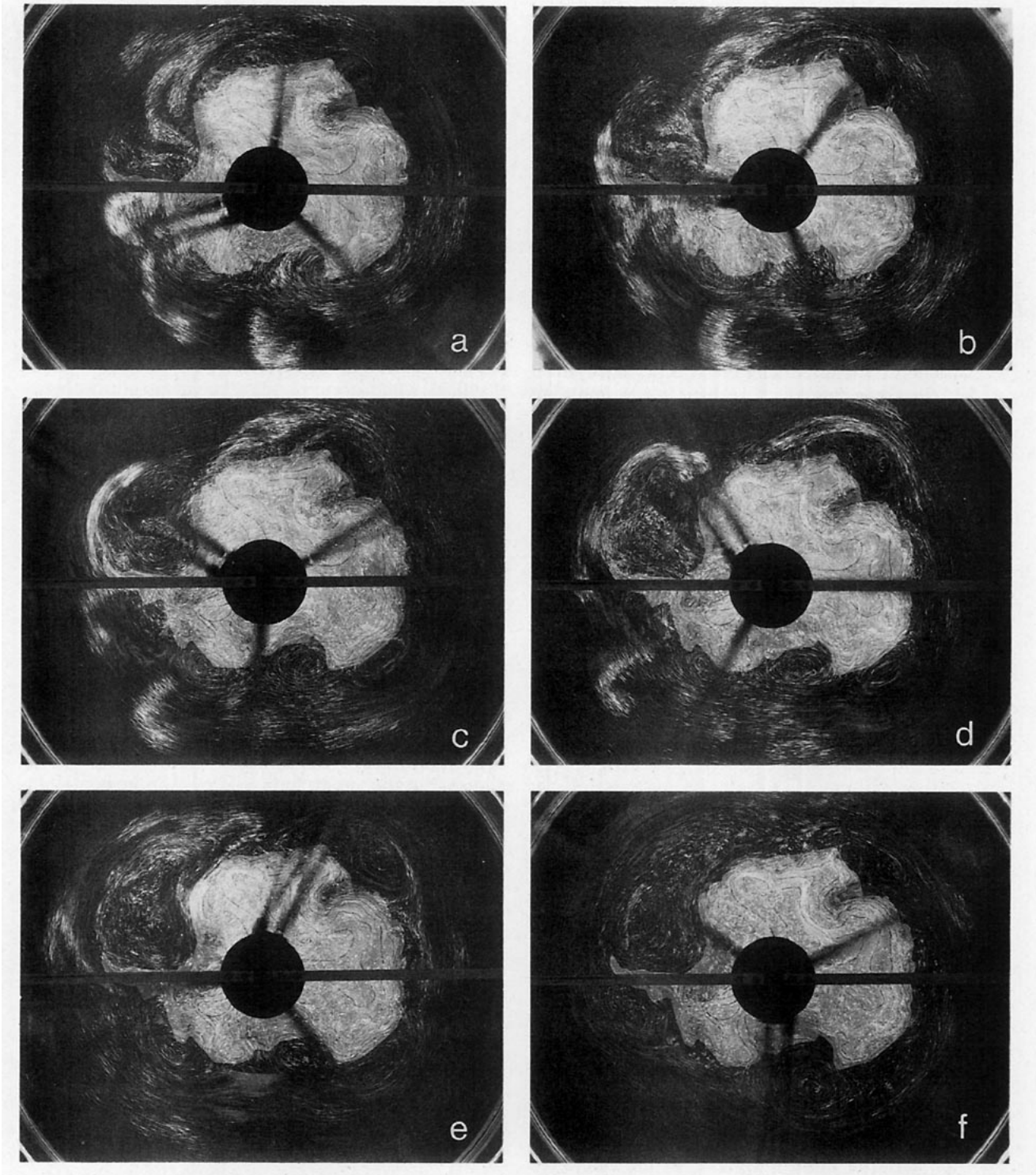

FIG. 7. Homogeneous fluid experiment for $\omega/\Omega = 0.03$, showing the flow field at a level slightly above the maximum topographic height. Very small beads are illuminated in a narrow laser beam. Tank rotation period is 4 seconds. The sequence denotes successive times after the commencement of relative motion of Antarctica, simulating westerly flow. The camera is rotating with the topography, and time exposures are 4 seconds: (a) $t = 12$ s (mean time), (b) $t = 22$ s, (c) $t = 32$ s, (d) $t = 42$ s, (e) $t = 62$ s, (f) $t = 122$ s, and (g) $t = 8$ min.

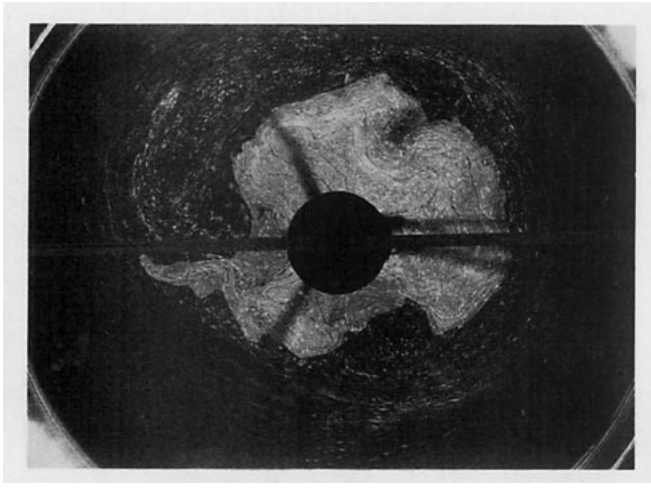

FIG. 7. (*Continued*)

values of $\omega/\Omega = 0.015$ and 0.06. The pattern of development with time, and the final steady state, are much the same as shown in Fig. 7, although the details vary. For $\omega/\Omega = 0.06$, for example, the anticyclonic eddy over eastern Antarctica is larger and stronger, whereas for $\omega/\Omega = 0.015$ it is not evident at all. Also, for $\omega/\Omega = 0.06$, the Weddell Sea eddy is extended downstream, almost to the Prydz Bay region.

These observations may be interpreted with the aid of the vorticity equation (3.4), which governs the low Rossby number variations that occur after the first few rotation periods. The strong vertical coupling due to rotation inhibits flow across topographic height contours and makes the flow nearly uniform with height. Flow around topographic irregularities may then separate and cause lee-side eddies, as in purely two-dimensional experiments. The process at low levels is analogous to the formation of eddies behind a bluff body (for example, a house) at large Reynolds number in nonrotating flows; in rotating flow the effect is then propagated vertically through the fluid by inertial waves.

Laboratory experiments on flow of homogeneous rotating fluid at small Rossby numbers past two-dimensional (no z-dependence) and three-dimensional obstacles attached to sidewalls have been described by Griffiths and Linden (1983). Boyer et al. (1987) have extended these observations to larger Rossby numbers for two-dimensional obstacles, and have examined the properties of lee-side eddies in more detail. For (conditions corresponding to) steady eastward flow past two-dimensional obstacles on a southern boundary with Southern Hemisphere rotation, Griffiths and Linden observed two types of lee-side flow pattern. The first consisted of continually shed eddies and occurred for $\mathrm{Ro} > 39E_v^{2/3}$, and the second consisted of a long and relatively stagnant wake, for $\mathrm{Ro} < 39E_v^{2/3}$, where $E_v = \nu/(2\Omega D^2)$. The Ro and E_v values of the present experiments lie above this boundary in the eddy-shedding region, but the E_v values are smaller (5×10^{-6}) than those of Griffiths and Linden, and the topographic features are irregular rather than symmetric. The stagnant wake pattern in the large-time limit resembles those described by Griffiths and Linden, but, as shown in the previous section, the free-surface beta-effect is important away from the topography. This appears to force the condition

$$\frac{\partial}{\partial\theta}[\text{flow properties}] \to 0, \qquad (4.1)$$

as steady state is approached, implying stagnant fluid poleward of the northernmost extent of the Antarctic Peninsula.

For comparison, some experiments were carried out with the same conditions as for Fig. 7, but with anticlockwise rotation of the tank. The flow patterns observed were substantially different. The westerly flow at the coast tended to follow the topographic contours, but some degree of separation was also observed at the major topographic features such as the Antarctic Peninsula, resulting in a fairly stagnant "eddy" in the Weddell Sea region. These observations reinforce the point that the direction of the flow in a rotating system is important for the character of separated flows.

b. Stratified experiments

The experiments described in section 4a for homogeneous fluids were repeated for uniformly stratified fluids with the same values of $\omega/\Omega = 0.015$, 0.03, and 0.06. We did not try to cover a range of stratification values, but chose a single value of the buoyancy frequency N (0.64 rad/sec) to give values of the parameters in Eqs. (3.13) and (3.14) which approximate the values in the atmosphere. The time development for $\omega/\Omega = 0.03$ is shown in Fig. 8. As in Fig. 7, Figs. 8a to 8f show the early structure on a time scale of several days to a month. Again, small cyclonic eddies forced by coastal irregularities dominate the early development. Disturbances over the topography are weak and the flow attains an approximate steady state earlier than in the homogeneous case (in about 45 s).

The "final" state shown in Fig. 8f is similar to that shown in Fig. 7g; the flow is dominated by eddies in the Weddell and Ross seas, Prydz Bay and the Bellingshausen Sea region, with stagnant fluid over the continent. There are no coastal eddies at other longitudes, so that "westerlies" are observed at the coast, in contrast to the barotropic case where coastal "easterlies" are found at most longitudes. As for Fig. 7, the prints in Fig. 8 contain information about the flow at the top of the fluid, in that beads on the free upper surface appear as broad grey streaks superimposed on the pattern of distinct white streaks of the lower illuminated layer. Again, the flow patterns at the two levels

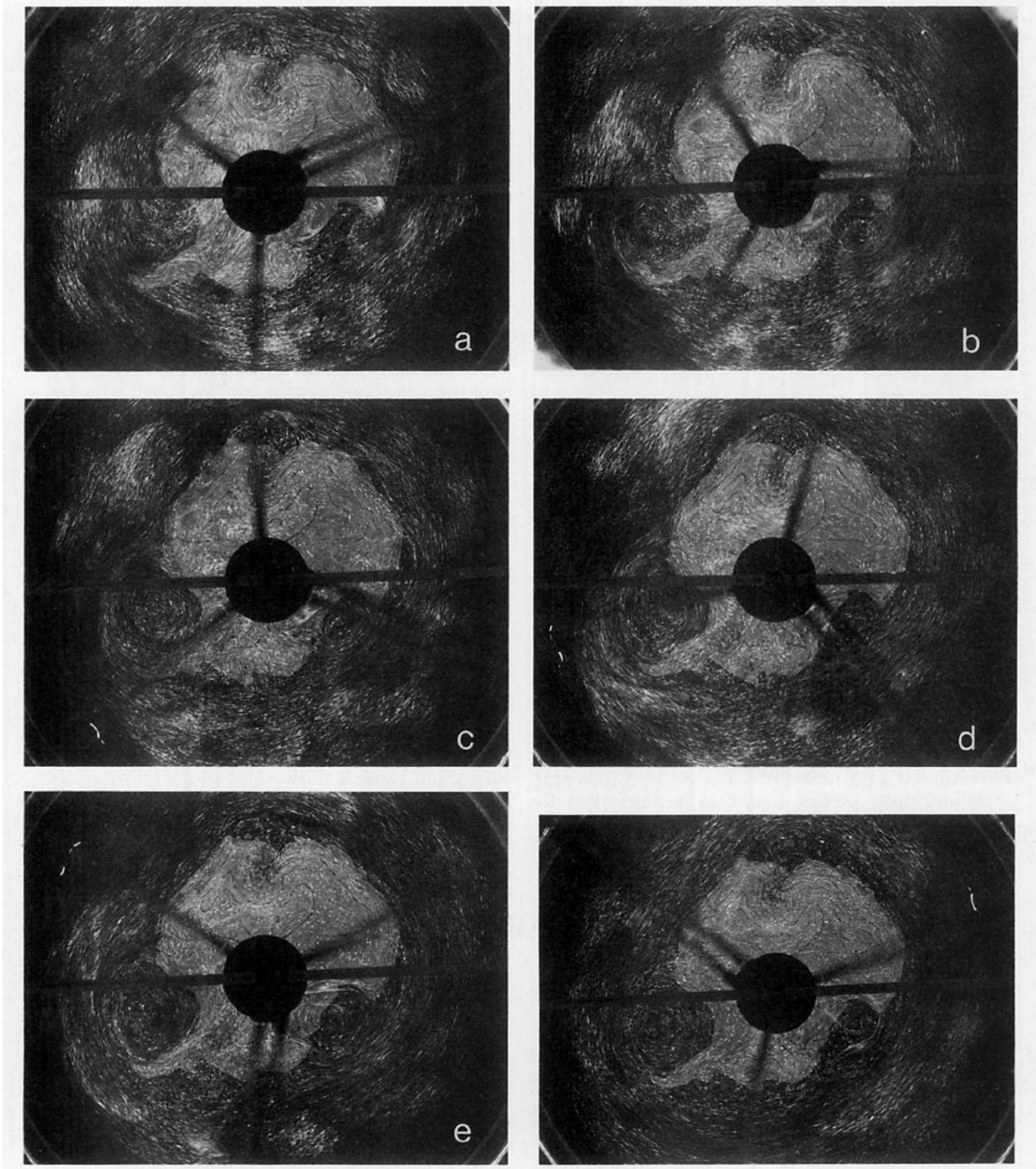

FIG. 8. As for Fig. 7 but with stratified fluid with buoyancy frequency $N = 0.64\ s^{-1}$: (a) $t = 12$ s, (b) $t = 22$ s, (c) $t = 32$ s, (d) $t = 42$ s, (e) $t = 62$ s, and (f) $t = 122$ s.

are very similar, indicating that the flow is essentially independent of depth, although the small-scale features are less distinct at the upper level.

The properties of the flow for the values $\omega/\Omega = 0.015, 0.06$ are generally similar to those shown in Fig. 8; the flow is dominated by the three main eddies,

and shows little variation with depth. Some localized changes were evident: in Fig. 8, the Antarctic Peninsula causes a substantial deflection to the flow, whereas for $\omega/\Omega = 0.015$ it acts as an almost total barrier, and for 0.06 it causes only a modest deflection of the flow over it. A Weddell Sea eddy is obtained in all three cases.

It should be emphasized that in all these cases, both homogeneous and stratified, the final "steady-state" flow is not completely steady because separated flows are essentially turbulent. Further, in the stratified case for $\omega/\Omega = 0.06$, at a late stage of the development the large eddy formed in the Ross Sea was shed and advected downstream. While this is an isolated incident in these experiments, the possibility of such major events occurring for other conditions after "steady state" has been reached cannot be discounted.

Most of the discussion for homogeneous fluids is also applicable, with appropriate changes, to the stratified case. Low Rossby number flows are governed by Eq. (3.8), where the vertical components of vorticity and density are the largest. The vertical length scale $2\Omega L/N$ is greater than the depth D of the fluid, so that in spite of the stratification the fluid is strongly coupled vertically by the pressure field. The flow again avoids crossing height contours, and hence separation occurs at coastal topographic features.

5. Comparison and discussion

If the mean flows at 700 and 850 mb shown in Figs. 2, 3 and 4 are compared with the "steady-state" flows in the experiments, namely Figs. 7g and 8f, a remarkable similarity is apparent. In all cases the center of the mean circumpolar vortex is displaced away from the pole towards the center of the eastern Antarctic land mass, at a longitude of approximately 75°E. This implies a wavenumber 1 perturbation on the vortex. In addition, the flow is dominated by three main eddies, in approximately the same locations in the experiments as in the atmospheric data, suggesting a wavenumber 3 structure over Antarctica. The only significant departure, perhaps, is in the Weddell Sea area, where in Fig. 2 the eddy appears to be centered further to the east. This is observed in all seasons at heights of 700 mb and below in the Le Marshall et al. dataset. In the other datasets of Hofmeyr (1957; in Fig. 3) and Jenne et al. (1974) (not shown), the center of the eddy is much closer to the Weddell Sea region and in conformity with the experiments, although the data of Jenne et al. do show a distinct eddy centered at about 30°E longitude for all months, which is consistent with Le Marshall et al. The variations may well be due to differences in analysis methods in such regions where data is sparse. In the experiments described, in the "steady state," an eddy was observed in this location for one set of conditions only ($\omega/\Omega = 0.06$).

This close correspondence between the experiments and observations provides very strong evidence that the mean atmospheric flow patterns are being directly forced by the substantial Antarctic topography, and that the same dynamical processes are occurring. The atmospheric mean flow is substantially barotropic (although the detail decreases with height, particularly above 500 mb), as are both the stratified and homogeneous experiments, so that in all cases the rotational constraint causes the flow to follow topographic contours over land, and to be virtually two-dimensional with flow separation over the sea. The circular boundary of the tank is expected to have a negligible effect on the flow because of its distance from the Antarctic topography and the near-zonal nature of the atmospheric flow at corresponding latitudes.

Given that we have potential vorticity conservation in both cases, another factor which appears to be important, on the basis of scaling, is the "beta effect." A steady solution to the inviscid barotropic vorticity equation on a beta-plane (or its laboratory equivalent) contains stagnant fluid poleward of the northernmost point of the Antarctic Peninsula. While this is not realized in the experiments, mainly because of the eddies, there is a pronounced tendency for velocities to be small inside this circle, in both the mean atmospheric flow and the steady-state experiments. It should be noted that the sloping free surface does not provide an accurate analogue for the beta effect for a stratified fluid, but this is not important here because the flow is mostly barotropic anyway.

Linearized topography cannot produce the same results; the topography must have sufficient height to deflect the flow and cause separation from coastal features. An attempt was made to observe topographic Rossby waves of the type described in the linear study of Egger and Fraedrich (1987), without success. This is not surprising since the forcing is steady in these experiments.

Another prominent feature of the observations is the high pressure region and anticyclonic circulation over eastern Antarctica. In the laboratory experiments this is broad and diffuse, if evident at all, and velocities over eastern Antarctica are very weak in the "steady state." This atmospheric feature may well be due to subsidence, a phenomenon that is not present in the laboratory experiments. Other features of the atmosphere that are not modeled here are the katabatic winds. These are difficult to model in the laboratory with real topography, although the attempt has been made (Gibson and Douglas 1969). James (1988) has suggested that the drainage flow circulation may force planetary waves which have a significant effect on the synoptic scale motions in the Southern Hemisphere, particularly at high latitudes. An estimate of the magnitude of the forcing of these effects may be obtained from the turnover time of this circulation: a drainage flow of 5 m s^{-1} (Parish and Bromwich 1986) with a depth of 100 m at 70°S causes a replacement of the poleward air in a time of about 2 years. This is long

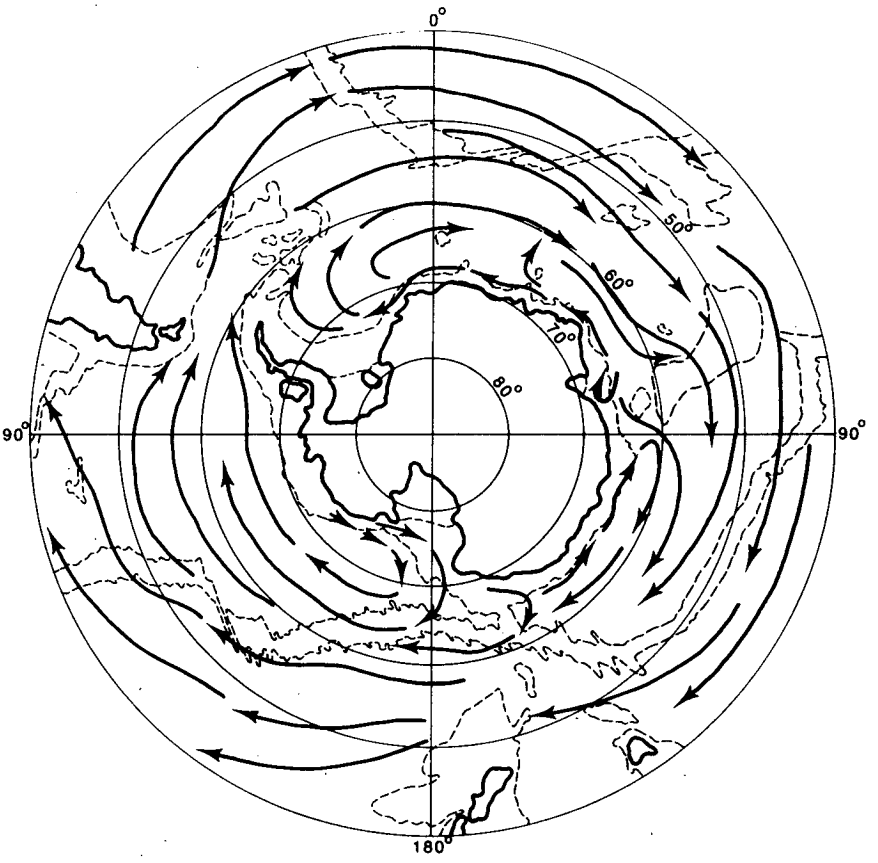

FIG. 9. General pattern of mean surface ocean drift from drifting buoy and iceberg data. The lengths of the lines represent about half-year displacements. The dashed lines show the 3000 m ocean depth contours (from Budd 1986).

when compared with the time taken for the air to circle the pole at 70°S at 5 m s^{-1} (from Fig. 6), which is about 32 days, and suggests that drainage effects are weak when compared with the effects described in this paper.

What is the effect of these topographic disturbances at lower latitudes? The displacement of the zonal jet due to wavenumber 1 is evident, but the wavenumber 3 pattern of the topographic eddies has the effect of smoothing out the indentations in the Antarctic coastline, so that the effect of these variations on the flow at lower latitudes is minimized.

Finally, we note that the observed pattern of surface drift in the oceans (Fig. 9) shows remarkable similarity to the atmospheric flows of Figs. 2 to 4, and the experimental flows of Figs. 7g and 8f. This is, perhaps, not surprising, since the ocean currents are expected to be driven by the mean wind stress. The latter causes an Ekman transport which produces a pressure field which in turn drives the current geostrophically in the same direction as the wind. Bottom topography will also exercise significant control over the ocean current pattern, in an analogous manner to that described here for the atmosphere.

Acknowledgments. The authors are most grateful to David Karoly for supplying the data for Figs. 2, 4 and 5, and numerous other charts from the Southern Hemisphere dataset of Le Marshall et al., and also to David Murray for constructing the model of Antarctica and skillfully conducting most of the experiments.

REFERENCES

Baines, P. G., 1987: Upstream blocking and airflow over mountains. *Ann. Rev. Fluid Mech.*, **19**, 75–97.

——, and P. A. Davies, 1980: Laboratory studies of topographic effects in rotating and/or stratified fluids. *Orographic Effects in Planetary Flows*, GARP Publications series No. 23, WMO, Geneva, 233–299.

Boyer, D. L., and R.-R. Chen, 1987: Laboratory simulation of mechanical effects of mountains on the general circulation of the Northern Hemisphere: Uniform shear background flow. *J. Atmos. Sci.*, **44**, 3552–3574.

——, ——, G. Chabert D'Hieres and H. Didelle, 1987: On the formation and shedding of vortices from side-wall mounted obstacles in rotating systems. *Dyn. Atmos. Oceans*, **11**, 59–86.

Budd, W. F., 1986: The Southern Hemisphere circulation of atmosphere, ocean and sea ice. *Second International Conference on Southern Hemisphere Meteorology*, Wellington, Amer. Meteor. Soc., 101–106.

Egger, J., and K. Fraedrich, 1987: Topographic Rossby waves over Antarctica. *Tellus*, **39A**, 110–115.

Gibson, T. T., and D. A. Douglas, 1969: Simulation of Antarctic circulations in a dishpan. *Weather,* **24,** 309–318.

Gill, A. E., 1982: *Atmosphere–Ocean Dynamics.* Academic Press, 662 pp.

Griffiths, R. W., and P. F. Linden, 1983: The influence of a side wall on rotating flow over bottom topography. *Geophys. Astrophys. Fluid Dyn.,* **27,** 1–33.

——, and ——, 1985: Intermittent baroclinic instability and fluctuations in geophysical situations. *Nature,* **316,** 801–803.

Hofmeyr, W. L., 1957: Upper air over the Antarctic. *Meteorology of the Antarctic* van Rooy, Ed., Weather Bureau, Pretoria, South Africa, 173–208.

James, I. N., 1988a: On the forcing of planetary scale Rossby waves by Antarctica. *Quart. J. Roy. Meteor. Soc.,* **114,** 619–638.

——, 1988b: Meteorology of a flat earth. *Nature,* **333,** 118.

Jenne, R. L., H. L. Crutcher, H. van Loon and J. J. Taljaard, 1974: A selected climatology of the Southern Hemisphere: computer methods and data availability. National Center of Atmospheric Research (NCAR), Boulder, CO, NCAR Tech. Note, NCAR-TN/STR-92, 92 pp.

Le Marshall, J. F., G. A. M. Kelly and D. J. Karoly, 1985: An atmospheric climatology of the Southern Hemisphere based on ten years of daily numerical analyses (1972–1982). Part I: Overview. *Aust. Meteor. Mag.,* **33,** 65–85.

Parish, T. R., and D. H. Bromwich, 1986: The inversion wind pattern over West Antarctica. *Mon. Wea. Rev.,* **114,** 849–860.

Pedlosky, J., 1979: *Geophysical Fluid Dynamics.* Springer Verlag, 624 pp.

Schwerdtfeger, W., 1984: *Weather and Climate of the Antarctic.* Elsevier, 261 pp.

Trenberth, K. E., 1979: Interannual variability of the 500 mb zonal mean flow in the Southern Hemisphere. *Mon. Wea. Rev.,* **107,** 1515–1524.